Damage-Mitigating Control of Mechanical Systems: Part I—Conceptual Development and Model Formulation[1]

Asok Ray
Fellow ASME

Min-Kuang Wu

Marc Carpino

Department of Mechanical Engineering,
The Pennsylvania State University,
University Park, PA 16802

Carl F. Lorenzo
NASA Lewis Research Center,
21000 Brookpark Road,
Cleveland, OH 44135

A major goal in the control of complex mechanical systems such as advanced aircraft, spacecraft, and power plants is to achieve high performance with increased reliability, availability, component durability, and maintainability. The current state-of-the-art of control systems synthesis focuses on improving performance and diagnostic capabilities under constraints that often do not adequately represent the dynamic properties of the materials. The reason is that the traditional design is based upon the assumption of conventional materials with invariant characteristics. In view of high performance requirements and availability of improved materials, the lack of appropriate knowledge about the properties of these materials will lead to either less than achievable performance due to overly conservative design, or over-straining of the structure leading to unexpected failures and drastic reduction of the service life. The key idea of the research reported in this paper is that a significant improvement in service life can be achieved by a small reduction in the system dynamic performance. This requires augmentation of the current system-theoretic techniques for synthesis of decision and control laws with governing equations and inequality constraints that would model the properties of the materials for the purpose of damage representation and failure prognosis. The major challenge in this research is to characterize the damage generation process in a continuous-time setting, and then utilize this information for synthesizing algorithms of robust control, diagnostics, and risk assessment in complex mechanical systems. Damage mitigation for control of mechanical systems is reported in the two-part paper. The concept of damage mitigation is introduced and a continuous-time model of fatigue damage dynamics is formulated in this paper which is the first part. The second part which is a companion paper presents the synthesis of the open-loop control policy and the results of simulation experiments for transient operations of a reusable rocket engine.

1 Introduction

A major goal in the control of complex mechanical systems such as advanced aircraft, spacecraft, and power plants is to achieve high performance with increased reliability, availability, component durability, and maintainability (Lorenzo and Merrill, 1991a; Ray et al., 1992a, 1992b). The specific requirements are:

- Extension of the service life of the controlled process;
- Increase of the mean time between major maintenance actions;
- Reduction of risk in the integrated control-structure-materials system design.

Therefore, control systems need to be synthesized by taking

[1]The research work reported in this paper is supported in part by: NASA Lewis Research Center under grant no. NAG 3-1240; National Science Foundation under Research grant no. ECS-9216386; Electric Power Research Institute under Contract EPRI RP8030-5; Office of Naval Research under grant no. N00014-90- J-1513; National Science Foundation under Research Equipment grant no. MSS-9112609.

Contributed by the Dynamic Systems and Control Division for publication in the JOURNAL OF DYNAMIC SYSTEMS, MEASUREMENTS, AND CONTROL. Manuscript received by the DSCD September 16, 1992; revised manuscript received April 20, 1993. Associate Technical Editor: J. Stein.

performance, mission objectives, service life, and maintenance and operational costs into consideration. The current state-of-the-art of control systems synthesis focuses on improving dynamic performance and diagnostic capabilities under the constraints that often do not adequately represent the material properties of the critical plant components. The reason is that the traditional design is based upon the assumption of conventional materials with invariant characteristics. In view of high performance requirements and availability of improved materials that may have significantly different damage characteristics relative to conventional materials, the lack of appropriate knowledge about the properties of these materials will lead to either of the following:

- Less than achievable performance due to overly conservative design; or
- Over-straining of the structure leading to unexpected failures and drastic reduction of the useful life span.

For example, reusable rocket engines present a significantly different problem in contrast to expendable propulsion systems that are designed on the basis of minimization of weight and acquisition cost under the constraint of specified system reliability. In reusable rocket engines, multiple start-stop cycles cause large thermal strains; and dynamic loads induce high cyclic strains leading to fatigue failures. The original design goal of the Space Shuttle Main Engine (SSME) was specified for 55 flights before any major maintenance, but the current practice is to disassemble the engine after each flight for maintenance (Lorenzo and Merrill, 1991a). Another example is design modification of the F-18 aircraft as a result of conversion of the flight control system from analog to digital, which would lead to a significant change in the load spectrum on the airframe structure. In this case, a major goal of the vehicle control systems redesign should be to achieve a trade-off between flight maneuverability, and durability of the critical components (Noll et al., 1991).

As the science and technology of materials continue to evolve, the design methodologies for damage-mitigating control must have the capability of easily incorporating an appropriate representation of material properties. This requires augmentation of the system-theoretic techniques for synthesis of decision and control laws with governing equations and inequality constraints that would model the mechanical properties of the materials for the purpose of damage representation and failure prognosis. The major challenge in this research is to characterize the damage generation process, and then utilize this information in a mathematical form for synthesizing algorithms of robust control, diagnostics, and risk assessment in complex mechanical systems.

Although a significant amount of research has been conducted in each of the individual areas of control and diagnostics and analysis and prediction of materials damage, integration of these two disciplines has not received much attention. In view of the integrated structural and flight control of advanced aircraft, Noll et al. (1991) have pointed out the need for interdisciplinary research in the fields of active control technology and structural integrity, specifically fatigue life analysis. Lorenzo and Merrill (1991a) have proposed a concept of damage mitigation and failure prognosis in the framework of reusable rocket engines for space propulsion as an augmentation to intelligent control and diagnostics. This intelligent control system is hierarchically structured in which the top level coordinates the major functions of life extending control, adaptive control, real-time diagnostics and prognostics, and sensor/actuator fault accommodation. The goal is to ensure safety and achieve the mission objectives while arbitrating the potentially conflicting requirements of optimum performance and structural durability. However, this concept of damage mitigation is not restricted to intelligent control and diagnostics, and can be applied to any system where structural durability is an important issue.

The discussions above evince the need for interdisciplinary research in prediction and mitigation of structural damage of the mechanical components as an augmentation to control and diagnostics in complex processes. From this perspective, the ongoing research reported in this paper is oriented toward the development of a methodology to achieve optimized trade-off between the system performance and structural durability of the plant under control. The task is to synthesize a robust control and diagnostic system by maintaining the damage of critical component(s) within prescribed limit(s) while allowing for external disturbances and uncertainties in modeling of plant dynamics and damage dynamics.

This paper is the first part of a two-part paper in damage-mitigating control, and is organized in four sections including the Introduction and two Appendices. A framework of the damage-mitigating control system is proposed in Section 2. A model of fatigue damage dynamics is derived in the continuous-time setting in Section 3. A nonlinear fatigue damage model is then developed as a modification of the linear model. An extension of this fatigue damage model to include the effects of creep and corrosion is outlined in Appendix A. An alternative approach to fatigue damage modeling is briefly described in Appendix B. This first part is summarized and concluded in Section 4.

2 The Damage-Mitigating Control System

The damage-mitigating control system (*DCS*), also referred to as life extending control system (Lorenzo and Merrill, 1991b), is intended to function independently or as an integral part of a hierarchically structured control system. The *DCS* may be centralized or distributed depending on the spatial location of the critical plant components and the overall objective of the mission. As stated earlier, the major challenge in this research is to characterize the damage generation process such that this information can be directly applied to synthesize the control law. Therefore, we will focus on the fundamental issue of formulating a generic structure of the *DCS* with the objective of optimizing the plant dynamic performance while simultaneously maintaining the accumulated damage and the damage rate of the critical plant component(s) within prescribed limits.

Figure 1 shows a conceptual view of the *DCS* where the plant model is a finite-dimensional state-space representation of the system dynamics (e.g., thermal-hydraulic dynamics of the space shuttle main engine or propulsion and aerodynamics of an aircraft). The estimated plant states are inputs to the structural model which, in turn, generate the necessary

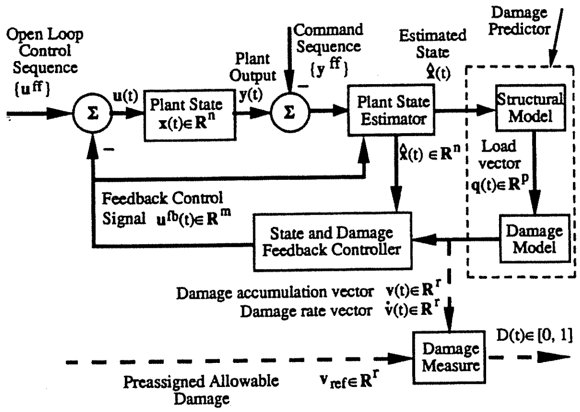

Fig. 1 A schematic diagram of the damage-mitigating control system

information for the damage model. The output of the structural model is the *load vector* which may consist of (time-dependent) stress, strain, temperature, wear, level of corrosion in gaseous and aqueous environments, and other physico-chemical process variables at the critical point(s) of the structure. The damage model is a continuous-time (instead of being a cycle-based) representation of life prediction such that it can be incorporated within the *DCS* model. The objective is to include the effects of damage rate and accumulated damage at the critical point(s) of the structure which may be subjected to time-dependent load. The damage state vector $v(t)$ could indicate the level of micro-cracking, macroscopic crack length, wear, creep, density of slip bands, etc., at one or more critical points, and its time derivative $\dot{v}(t)$ indicates how the instantaneous load is affecting the structural components. The overall damage $D(t)$ is a scalar measure of the combined damage at the critical point(s) resulting from (possibly) different sources (e.g., fatigue, creep, corrosion, or wear) relative to the preassigned allowable level v_{ref} of the damage vector. Although $D(t)$ may not directly enter the feedback or feedforward control of the plant, it can provide useful information for intelligent decision-making such as damage prognosis and risk analysis.

The plant dynamics and damage estimator in Fig. 1 are modeled by nonlinear (and possibly time-varying) differential equations which must satisfy the local Lipschitz condition (Vidyasagar, 1992) within the domain of the plant operating range. The structural model in Fig. 1 consists of solutions of structural dynamic equations representing the (mechanical and thermal) load conditions. A general structure of the plant and damage dynamics and their constraints is represented in the deterministic setting as follows:

Task Period: Starting time t_0 to final time t_f

Plant dynamics:

$$\frac{dx}{dt} = \mathrm{f}(x(t),u(t),t);\ x(t_0) = x_0;\ \text{and}$$

$$y(t) = g(x(t).u(t),t) \quad (1)$$

Damage dynamics:

$$\frac{dv}{dt} = h(v(t),q(x,t),t);\ v(t_0) = v_0;\ h \geq 0\ \forall t \quad (2)$$

Damage measure:

$$D(t) = \xi(v(t),v_{\text{ref}}) \text{ and } D(t) \in [0,1] \quad (3)$$

Damage rate tolerance:

$$0 \leq h(v(t),q(x,t),t) < \beta(t)\ \forall t \in [t_0,t_f] \quad (4)$$

Accumulated damage tolerance:

$$[v(t_f) - v(t_0)] < \Gamma \quad (5)$$

where (see also Fig. 1)

$x \in \mathbf{R}^n$ is the plant state vector;
$\hat{x} \in \mathbf{R}^n$ is the estimated plant state vector;
$y \in \mathbf{R}^k$ is the plant output vector;
$y^{ff} \in \mathbf{R}^k$ is the reference plant output vector;
$u \in \mathbf{R}^m$ is the control input vector;
$u^{ff} \in \mathbf{R}^m$ is the reference control input vector;
$v \in \mathbf{R}^r$ is the damage state vector;
$v_{\text{ref}} \in \mathbf{R}^r$ is the preassigned limit for the damage state vector;
$\beta(t) \in \mathbf{R}^r$ and $\Gamma \in \mathbf{R}^r$ are specified tolerances for the damage rate and accumulated damage, respectively;
$q \in \mathbf{R}^p$ is the load vector; and
$D \in [0,1]$ is a scalar measure of the accumulated damage.

The vector differential Eqs. (1) and (2) become stochastic if the randomness of plant and material parameters is included in the models, or if the plant is excited by discrete events occurring at random instants of time (Sobczyk and Spencer, 1992). The stochastic aspect of damage-mitigating control is a subject of future research.

The proposed *DCS* in Fig. 1 uses the concept of conventional state estimation and state feedback together with the information of damage rate and accumulated damage to generate an appropriate feedback control signal. Although this additional information renders the control system to be highly nonlinear, the dynamic performance and service life of the plant can be better managed with damage mitigation. Without the damage feedback, the controller depicted in Fig. 1 would reduce to a conventional output feedback controller such as Linear Quadratic Gaussian (LQG) (Kwakernaak and Sivan, 1972). Although the details of *DCS* design are not addressed in this two-part paper, an open-loop control policy has been formulated in the second part (Ray et al., 1994).

3 Modeling of Damage Dynamics

Damage of mechanical structures is usually a result of fatigue, creep, corrosion, and their combinations (Courtney, 1990; Suresh, 1991). The prime focus of the research reported in this paper is representation of fatigue damage in the continuous-time setting. However, experimental results indicate that, in many materials, reduction of fatigue life at elevated temperatures (as low as 30 percent of the melting point in some cases) is significantly influenced by gaseous and aqueous environments. While the fatigue damage is cycle-dependent, the creep damage and corrosion damage are time-dependent. As discussed earlier, a time-dependent model of damage dynamics, having the structure of Eq. (2), is necessary for analysis and synthesis of *DCS*. From this perspective, a dynamic model of fatigue damage has been formulated in the continuous-time setting. Although this damage model has a deterministic structure, it can be recast in the stochastic setting to include the effects of both unmodeled dynamics and parametric uncertainties. Augmentation of the fatigue damage model to include dynamics of corrosion and creep damage is briefly discussed in Appendix A.

Because of the wide ranges in mechanical properties of materials, extensive varieties of experiments have been conducted for fatigue analysis, and many models have been proposed for fatigue life prediction in aerospace and ground vehicles (Newman, 1981; Tucker and Bussa, 1977). Each of these models expresses the damage dynamics by an equation with the number of cycles N as the independent variable. In contrast, the damage dynamics in Eq. (2) are expressed as a vector differential equation with respect to time, t, as the independent variable. The advantages of this approach are that it allows the damage model to be incorporated within the constrained optimization problem and that the damage accumulated between any two instants of time can be derived even if the stress-strain hysteresis loop is not closed. This concept is applicable to different models of damage dynamics such as those resulting from cyclic strain or crack propagation. To this effect, we propose to model the continuous-time dynamics of fatigue damage based on the following two approaches.

- Cyclic Strain-Life: In this approach, the local stress-strain behavior is analyzed at certain critical points where failure is likely to occur (Dowling, 1983). The local strain may be directly measured from a strain gauge, or computed via finite element analysis. The local stress is estimated from the cyclic stress-strain curve. A cycle-based approach is then used to estimate the fatigue damage from the strain-life curves at different levels of stress and strain in the load history. We propose to determine the damage accumulation within a cycle using the classical Palmgren-Miner rule and subsequently modify it via the damage curve approach of Bolotin (Bolotin, 1989; Sobczyk and Spencer, 1992).
- Linear Elastic Fracture Mechanics (LEFM): The LEFM approach is built upon the concept of a physical measure of damage in terms of the crack length and the size of the plastic zone at the crack tip (Wheeler, 1971; Willenborg, 1972). The accumulated damage is computed by integrating the crack growth rate over the number of cycles. This is based on the crack growth rate equation being approximated by an exponential function of stress intensity factor range of the component (Bannantine et al., 1990). The component is assumed to fail when the crack reaches the critical length which, in turn, is determined from the fracture toughness of the component on the basis of experimental data.

While the primary approach adopted in this paper is based on cyclic strain-life for developing a continuous-time damage model, an alternative approach based on the LEFM concept is presented in Appendix B.

3.1 Damage Modeling Based on the Cyclic Strain-Life Concept. The cyclic strain-life approach recognizes that the fatigue life is primarily controlled by the local strain at the critical point(s) of the component. The first goal is to model linear damage accumulation in the continuous-time setting. Referring to Fig. 2, let the point O be the starting point of a reversal, let A and B be two consecutive points on the same rising reversal, and let N_A and N_B represent the total number of cycles to failure with constant load amplitudes, OA/2 and OB/2, respectively. Then, the half-cycle increment of the linear accumulated damage δ between points A and B is defined as:

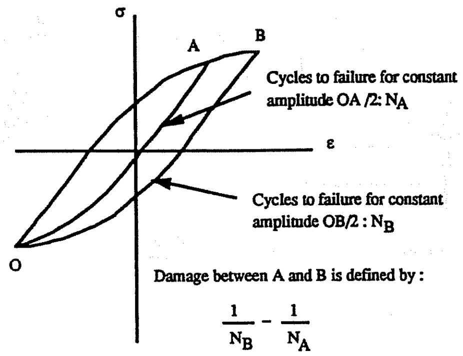

Fig. 2 Damage between two points on the same reversal

$$\Delta\delta_{A,B} = \frac{1}{N_B} - \frac{1}{N_A} \tag{6}$$

In Eq. (6), it is assumed that the damage occurs only on the rising reversal, i.e., if the stress is monotonically increasing, and no damage occurs during unloading, i.e., if the stress is monotonically decreasing. This assumption is consistent with the physical phenomena observed in the fatigue crack propagation process. Given that $\Delta\sigma$ is the stress increment between point A and point B, the average damage rate with respect to this stress change is equal to $\Delta\delta/\Delta\sigma$. Let Δt be the time interval from A to B, the average rate of linear damage δ in terms of the stress σ can be transformed into the time domain by $\Delta\delta/\Delta t = (\Delta\delta/\Delta\sigma) \times (\Delta\sigma/\Delta t)$. Making Δt infinitesimally small, the instantaneous damage rate becomes

$$\frac{d\delta}{dt} = \lim_{\Delta t \to 0} \frac{\Delta\delta}{\Delta\sigma} \times \frac{\Delta\sigma}{\Delta t} = \frac{d\delta}{d\sigma} \times \frac{d\sigma}{dt} \tag{7}$$

where the instantaneous stress rate $d\sigma/dt$ can be generated from direct measurements of strain rate or the finite element analysis, and $d\delta/d\sigma$ is derived from the existing cycle-based formulae (Bannantine et al., 1990). The life prediction formula (Dowling, 1983) and the cyclic stress-strain relationship are used to evaluate $d\delta/d\sigma$ in Eq. (7). Replacing N_f by $1/\Delta\delta$ where $\Delta\delta$ represents the increment in linear damage δ during one cycle, the standard strain life relationship can be written as:

$$\frac{|\epsilon - \epsilon_r|}{2} = \left(\frac{\sigma_f' - \sigma_m}{\mathrm{E}}\right)\left(\frac{\Delta\delta}{2}\right)^{-b} + \epsilon_f'\left(1 - \frac{\sigma_m}{\sigma_f'}\right)^{\frac{c}{b}}\left(\frac{\Delta\delta}{2}\right)^{-c} \tag{8}$$

where ϵ_r is the total strain corresponding to the reference stress σ_r at the starting point R of a given reversal as determined from the rainflow cycle counting method: $|\epsilon - \epsilon_r|/2$ is the strain amplitude between the current point and the reference point; and the fatigue strength coefficient σ_f', fatigue strength exponent b, fatigue ductility coefficient ϵ_f'

and fatigue ductity exponent c are experimentally evaluated parameters of the material. The above equation does not provide a closed form solution for the predicted damage $\Delta\delta$. The general approach to solve this problem is to separate Eq. (8) into two different modes. The first term on the right side corresponds to the so called elastic damage increment $\Delta\delta_e$ and the second term corresponds to the so called plastic damage increment $\Delta\delta_p$. These two damage increments, $\Delta\delta_e$ and $\Delta\delta_p$, can be derived separately in an explicit form. Generally speaking, for high cycle fatigue, the elastic damage yields more accurate prediction than the plastic damage, and vice versa for low cycle fatigue. Therefore, the predicted damage increment $\Delta\delta$ should be obtained as a weighted average of $\Delta\delta_e$ and $\Delta\delta_p$ where the weights depend on the relative accuracy of the elastic and plastic modes of damage computation under the current load condition. The elastic strain, ϵ_{re}, and the plastic strain, ϵ_{rp}, corresponding to the reference stress, σ_r, are defined as:

$$\epsilon_{re} = \frac{\sigma_r}{E} \quad \text{and} \quad \epsilon_{rp} = \epsilon_r - \epsilon_{re} \tag{9}$$

Equation (8) can be split into the elastic damage mode and plastic damage mode as:

$$\frac{|\epsilon_e - \epsilon_{re}|}{2} = \frac{\sigma_f' - \sigma_m}{\mathrm{E}}\left(\frac{\Delta\delta_e}{2}\right)^{-b} \tag{10a}$$

$$\frac{|\epsilon_p - \epsilon_{rp}|}{2} = \epsilon_f'\left(1 - \frac{\sigma_m}{\sigma_f'}\right)^{\frac{c}{b}}\left(\frac{\Delta\delta_p}{2}\right)^{-c} \tag{10b}$$

where $\mathrm{sgn}(\epsilon_e - \epsilon_{re}) = \mathrm{sgn}(\epsilon_p - \epsilon_{rp})$; and the elastic and plastic strain amplitudes, $|\epsilon_e - \epsilon_{re}|/2$ and $|\epsilon_p - \epsilon_{rp}|/2$, are related to the state of stress following the cyclic stress-strain characteristics:

$$\frac{|\epsilon_e - \epsilon_{re}|}{2} = \frac{|\sigma - \sigma_r|}{2E} \tag{11a}$$

$$\frac{|\epsilon_p - \epsilon_{rp}|}{2} = \left(\frac{|\sigma - \sigma_r|}{2K'}\right)^{\frac{1}{n'}} \tag{11b}$$

where n' is the cyclic strain hardening exponent and K' is the cyclic strength coefficient. It is well known (Bannantine, 1990) that n' and K' are equal to b/c and $\sigma_f'/((\epsilon_f')^{b/c})$, respectively. From Eqs. (10a), (10b), (11a), and (11b), the closed form solutions for δ_e and δ_p can be obtained in terms of stress instead of strain as given below:

$$\delta_e = 2\times\left(\frac{|\sigma - \sigma_r|}{2(\sigma_f' - \sigma_m)}\right)^{-\frac{1}{b}} \tag{12a}$$

$$\delta_p = 2\times\left(\frac{1}{\epsilon_f'}\times\left(\frac{|\sigma - \sigma_r|}{2K'}\right)^{\frac{1}{n'}}\times\left(1 - \frac{\sigma_m}{\sigma_f'}\right)^{-\frac{c}{b}}\right)^{-\frac{1}{c}} \tag{12b}$$

Step changes in the reference stress σ_r can occur only at isolated points in the load spectrum. Since the damage increment is zero at any isolated point, the damage accumulation can be evaluated at all points excluding these isolated points which constitute a set of zero Lebesgue measure (Royden, 1988). Exclusion of the points of step changes in σ_r does not cause any error in the computation of damage, and $d\sigma_r/dt$ can be set to zero because σ_r is piecewise constant. Further, since it is assumed that no damage occurs during unloading, the damage rate can be made equal to zero when $\sigma < \sigma_r$. The elastic damage rate $d\delta_e/dt$ and the plastic damage rate $d\delta_p/dt$ are computed by differentiating Eqs. (12a) and (12b).

If $\sigma \geq \sigma_r$, then

$$\frac{d\delta_e}{dt} = 2\times\frac{d}{d\sigma}\left(\left(\frac{\sigma - \sigma_r}{2(\sigma_f' - \sigma_m)}\right)^{-\frac{1}{b}}\right)\times\frac{d\sigma}{dt}, \text{ and} \tag{13a}$$

$$\frac{d\delta_p}{dt} = 2\times\frac{d}{d\sigma}\left(\left(\frac{1}{\epsilon_f'}\times\left(\frac{\sigma - \sigma_r}{2K'}\right)^{\frac{1}{n'}}\times\left(1 - \frac{\sigma_m}{\sigma_f'}\right)^{-\frac{c}{b}}\right)^{-\frac{1}{c}}\right)\times\frac{d\sigma}{dt}; \tag{13b}$$

else $d\delta_e/dt = 0$ and $d\delta_p/dt = 0$.

The damage rate $d\delta/dt$ is obtained as the weighted average of the elastic and plastic damage rates such that

$$\frac{d\delta}{dt} = w\frac{d\delta_e}{dt} + (1 - w)\frac{d\delta_p}{dt} \tag{14}$$

where the weighting function, w, is based on the elastic and plastic strain amplitudes in Eqs. (10a) and (10b) as:

$$w = \frac{\epsilon_e - \epsilon_{re}}{\epsilon - \epsilon_r} \quad \text{and} \quad 1 - w = \frac{\epsilon_p - \epsilon_{rp}}{\epsilon - \epsilon_r} \tag{15}$$

Equations (13) to (15) are then used to obtain the damage rate at any instant. The damage increment between two consecutive points t_k and t_{k+1} on the same reversal can be calculated by integrating the damage differential $d\delta$.

The continuous-time damage model in Eqs. (13) to (15) is derived on the basis of linear damage accumulation following the Palmgren-Miner's rule. Although this concept of linear damage accumulation has been widely used due to its simplicity in computation, the cumulative damage behavior is actually nonlinear (Bolotin, 1989; Suresh, 1991). Experimental results show that, for variable amplitude loading, the accumulated damage is dependent on the order in which the load cycles are applied. This phenomenon is known as the sequence effect which is further explained in the next section. Since the structural components of complex mechanical systems are subjected to loads of varying amplitude, the linear rule of damage accumulation which is commonly used for fatigue life assessment could lead to erroneous results due to this sequence effect. Therefore, a nonlinear damage rule needs to be established for accurate prediction of the damage rate and damage accumulation in the critical components.

3.2 Modeling of Nonlinear Cumulative Damage Using the Damage Curve Approach. The concept of a nonlinear damage curve to represent the damage was first conceived by Marco and Starkey (1954). No mathematical representation of damage curve was proposed at that time because the physical process of damage accumulation was not adequately understood. Manson and Halford (1981) pro-

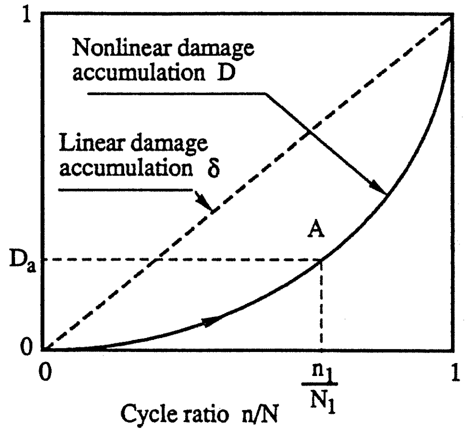

Fig. 3 Nonlinear damage curve under constant amplitude loading

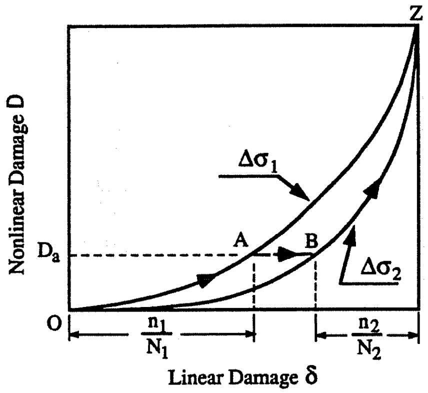

Fig. 4 Nonlinear damage accumulation ($\Delta\sigma_1 > \Delta\sigma_2$)

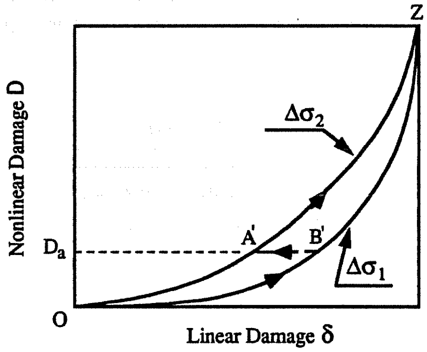

Fig. 5 Nonlinear damage accumulation ($\Delta\sigma_1 < \Delta\sigma_2$)

posed the double linear rule primarily based on the damage curve approach for treating cumulative fatigue damage. In their paper, an effort was made to mathematically represent the damage curve and approximate it by two piecewise line segments. The total fatigue life was then divided into two phases so that the linear damage rule can be applied in each phase of the life. A concept similar to the damage curve approach was proposed by Bolotin (1989) with a mathematical representation which does not necessarily assess the damage on the basis of cycles and is more appropriate for modeling in the continuous-time setting. Therefore, we have adopted Bolotin's approach in this research to develop a continuous-time model of nonlinear damage accumulation. A review of the damage curve approach following Bolotin's nonlinear damage equation is presented below.

Figure 3 shows a comparison of the accumulations of linear damage, δ, and nonlinear damage, D, as a function of the cycle ratio, n/N, where n is the actual number of cycles undergone and N is the number of cycles to failure under a constant amplitude loading. The damage accumulates along the curve as the loading cycles are applied. For example, if n_1 cycles of a constant stress amplitude, which as a fatigue life of N_1, are applied to the component, the accumulated damage will follow the curve and reach D_a as indicated in Fig. 3 where the abscissa is the normalized cycle ratio with respect to its fatigue life and the ordinate is the physical damage accumulation of the component. Bolotin (1989) used the following analytical relationship between D and δ:

$$D = (\delta)^{\gamma(\sigma_a)} \tag{16}$$

where the exponent γ describes the nonlinearity of the curve and usually is a function of the stress amplitude σ_a. Equation (16) indicates that the nonlinear damage accumulates along different curves under different stress amplitudes. Generally speaking, for high-strength materials that usually strain soften (Hertzberg, 1989), a smaller stress amplitude tends to make the damage curve more nonlinear, i.e., increase the γ- parameter. The notion of nonlinear damage accumulation via the damage curve approach and how it is related to the sequence effect under varying stress amplitude are explained in the following example.

Let a smooth specimen be subjected to two levels of stress amplitude, $\Delta\sigma_1$ and $\Delta\sigma_2$ (say $\Delta\sigma_1 > \Delta\sigma_2$), with respective fatigue lives of N_1 and N_2 cycles ($N_1 < N_2$). Let OAZ and OBZ be the nonlinear damage curves for cyclic loads of stress amplitudes $\Delta\sigma_1$ and $\Delta\sigma_2$, respectively, as shown in Fig. 4. If n_1 cycles of $\Delta\sigma_1$ are applied prior to $\Delta\sigma_2$, then the damage accumulation up to the point A along the curve OAZ is equal to D_a. Then, let $\Delta\sigma_2$ be applied for n_2 cycles when the specimen fails. The damage accumulation, in this process, continues from its present state D_a at B along the curve OBZ until the nonlinear damage reaches 1 at Z. The linear rule would underestimate the damage by $(1 - n_1/N_1 - n_2/N_2)$ which is equal to the length AB as indicated in Fig. 4. Next consider the reverse situation in Fig. 5 where $\Delta\sigma_2$ is applied first for n_2' cycles followed by $\Delta\sigma_1$ for n_1' cycles when the specimen fails. The linear rule, in this case, overestimates the damage by $(n_1'/N_1 + n_2'/N_2 - 1)$ which is the length $A'B'$ as shown in Fig. 5.

The above example illustrates the basic concept of the damage curve approach. For multiple-level loading, the same procedure can be applied by first identifying the current damage state and then following the damage curve associated with the current loading condition. If a component is subjected to spectral loading, then the techniques of cycle-counting, prediction of linear damage increments, and computation of nonlinear damage via the damage curve approach need to be integrated into a single procedure.

In the damage curve approach described above, the γ-parameter is usually assumed to be dependent solely on the stress amplitude level (Manson and Halford, 1981). High-strength materials such as 4340 steel usually yield very large

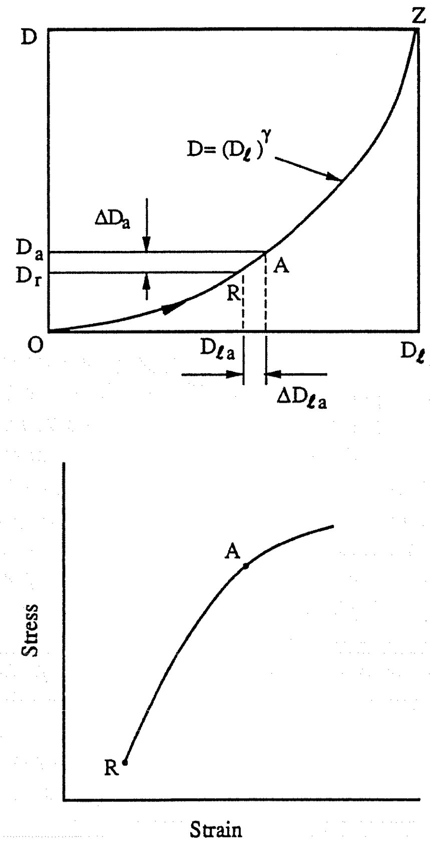

Fig. 6 Nonlinear damage increments

values of γ especially under high-cycle fatigue. From Eq. (16), it follows that a large γ initially creates a very small damage, which could be out of the range of precision of the computer. This necessitates formulation of a computationally practical method of damage prediction. It follows from a crack propagation model such as the Paris model (Paris and Erdogan, 1963) that the crack growth rate is dependent not only on the stress amplitude but also on the current crack length. Recognizing the fact that the crack itself is an index of accumulated damage, it is reasonable to assume the γ-parameter to be dependent on both stress amplitude and the current level of damage accumulation, i.e., $\gamma = \gamma(\sigma_a, D)$. Therefore, we propose the following modification of Eq. (16):

$$D = (\delta)^{\gamma(\sigma_a, D)} \tag{17}$$

where D and δ are the current states of nonlinear and linear damage accumulation, respectively. Although the above Eq. (17) has an implicit structure, it can be solved via a recursive relationship.

The next part of this section describes a modification of the damage curve approach to develop a nonlinear damage model in the continuous-time setting. Following the concept of the linear damage model in the continuous-time setting, the nonlinear damage at any point on a rising reversal can be obtained as explained below.

Referring to the bottom part of Fig. 6, let A be any point on the rising reversal and R be its reference point as determined from the rainflow cycle counting method (Dowling, 1983). Let the current state of damage at the reference point R be equal to D_r and let ORAZ be the damage curve associated with the stress amplitude $RA/2$ as shown in the top part of Fig. 6. Corresponding to the nonlinear damage D_r, we bring in the notion of the "virtual" linear damage, δ_a, at the point R as follows:

$$\delta_a = (D_r)^{\frac{1}{\gamma_r^a}} \tag{18}$$

where γ_r^a is the γ-parameter associated with the stress amplitude $RA/2$ and nonlinear accumulated damage D_r at R. The term "virtual" means that δ_a is the linear damage which would be incurred if the component had been subjected to the cyclic stress of constant amplitude, $RA/2$, from its initial damage state to the current damage state at R. Similar to γ_r^a in Eq. (18), we define γ_a^a as the γ-parameter associated with the damage state D_a at the point A. Referring to Fig. 6, the functional relationships among D_a, D_r and the corresponding γ-parameters γ_a^a and γ_r^a are defined as follows:

$$\begin{cases} \gamma_a^a = \gamma(\sigma_a, D_a) \\ D_a = (\delta_a + \Delta\delta_a)^{\gamma_a^a} \end{cases} \text{and} \begin{cases} \gamma_r^a = \gamma(\sigma_a, D_r) \\ D_r = (\delta_a)^{\gamma_r^a} \end{cases} \tag{19}$$

where σ_a is the stress amplitude $RA/2$, and $\Delta\delta_a$ is the linear damage increment between R and A obtained via the procedure described in Section 3.1. The damage D_r in the right part of Eq. (19) represents the damage state at the reference point R and therefore its value is already computed from the past load history. Having known D_r, the γ-parameter γ_r^a and the "virtual" linear damage δ_a at R for the stress amplitude $RA/2$ can be evaluated from the right hand part of Eq. (19). The two unknowns, D_a and γ_a^a, which represent the damage state at the current point A, are computed by solving the equation pair in the left part of Eq. (19), and the issue of existence and uniqueness of the solution is discussed later in this section. Now, the (nonlinear) damage increment from the point R to A in Fig. 6 can be computed as:

$$\Delta D_a = D_a - D_r = (\delta_a + \Delta\delta_a)^{\gamma_a^a} - \delta_a^{\gamma_r^a} \tag{20}$$

In summary, the accumulated damage at any point within a reversal can be obtained by solving the following nonlinear equations:

$$\gamma = \gamma(\sigma_a, D) \tag{21}$$

$$D = (\delta + \Delta\delta)^{\gamma} \tag{22}$$

where δ is the "virtual" linear damage at the reference point and $\Delta\delta$ is the linear damage increment for the stress amplitude σ_a relative to the reference point.

The pair of Eqs. (21) and (22) does not have a closed form solution and therefore needs to be solved by an iterative method. However, an iterative solution at every point in the load history may not be practical from the perspective of computational efficiency. An efficient approach of obtaining a numerical solution would operate on a set of discrete points in the load history such that there is only a very small increment of damage between two consecutive points. Thus, both Eqs. (21) and (22) can be treated as linear line segments between the points R and A. This assumption is valid during the entire loading history with the possible exception of very low-cycle fatigue. One more interesting observation is that the γ-parameter is generally a monotonically increasing

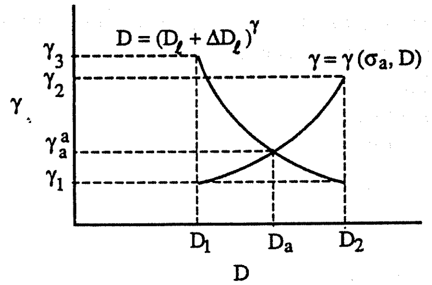

Fig. 7 Computation of nonlinear cumulative damage

function of the nonlinear damage D. This can be interpreted from the Paris equation that the growth rate of a macrocrack becomes larger as the crack length increases. Therefore, the damage rate would be larger at a higher degree of nonlinearity, which implies a larger value of γ. This phenomenon, however, may not be true if the stress intensity factor range is below the long crack threshold or if the material strain hardens. For the general case of $\gamma > 1$ (e.g., high strength materials that usually strain soften (Hertzberg, 1989)), γ is a monotonically increasing function of D in Eq. (21) and D is a monotonically decreasing function of γ in Eq. (22). Therefore, a unique solution of D and γ exists for the equation pair (21) and (22) as seen in Fig. 7. Similarly, a unique solution also exists if γ is less than 1 (e.g., ductile materials that usually strain harden) although the characteristics of both Eqs. (21) and (22) could be reversed.

Having computed the linear damage δ and linear damage increment $\Delta\delta$, a procedure for solving Eqs. (21) and (22) to obtain the nonlinear damage, D, is described below:

1. Let $D_1 = D_r$ and $\gamma_1 = \gamma_r$.
2. Compute $D_2 = (\delta + \Delta\delta)^{\gamma_1}$ from Eq. (22) and $\gamma_2 = \gamma(\sigma_a, D_2)$ from Eq. (21).
3. Compute $\gamma_3 = \gamma_1 \times \dfrac{\log \delta}{\log(\delta + \Delta\delta)}$ from Eqs. (17) and (21).
4. Find D_a in Fig. 7, which is approximated as the point of intersection of two straight line segments:

$$D_a = \frac{D_1(\gamma_2 - \gamma_1) + D_2(\gamma_3 - \gamma_1)}{\gamma_3 + \gamma_2 - 2\gamma_1} \tag{23}$$

The above procedure computes the nonlinear accumulated damage at any point on the rising reversal. If the stress is monotonically decreasing, there is no damage increment as described in Eqs. (13) to (14) for the case of linear damage accumulation. Finally, the rate of nonlinear damage accumulation is obtained directly by differentiating Eq. (17) with respect to time t:

$$\frac{dD}{dt} = \gamma(\delta)^{\gamma-1} \times \frac{d\delta}{dt} + (\delta)^{\gamma} \ln \delta \times \frac{d\gamma}{dt}. \tag{24}$$

3.3 The γ-Parameter Fitting for the Nonlinear Cumulative Damage Model. One major task in the above approach is to identify a mathematical representation for the γ-parameter as a function of the stress amplitude and the current damage state. It requires knowledge of the physical process of damage accumulation which may be obtained from either experimental data or a combination of experimental data and analysis, and an appropriate definition of damage. The γ-parameters are different, in general, for different materials and follow different structures of the governing equations. Furthermore, because the mechanisms attributed to the damage accumulation at various stages of fatigue life are different, no single approach apparently provides a sufficiently accurate prediction of damage throughout the fatigue life of a component. It is difficult, if not impossible, to construct a single structure for representation of γ. An alternative approach is to evaluate γ by interpolation. Once the damage is appropriately defined, and an analytical method for damage prediction is selected, the information needed for the nonlinear damage model can be generated via experimentation or analysis for a set of constant stress amplitudes. The values of γ are then computed by Eq. (21) for a given stress amplitude and the damage data ranging from the initial damage state D_0 to the failure condition at $D = 1$. The generated data, γ versus D, are then plotted for various amplitudes of stresses. These curves can be either fitted by nonlinear equations, if possible, or as linear piecewise representations. Since it is not practical to perform experiments at infinitesimally small increments of stress amplitude, γ can be only experimentally evaluated at selected discrete levels of stress amplitude. The values of γ for other stress amplitudes can then be interpolated. Since the characteristics of γ may strongly depend on the type of the material, availability of pertinent experimental data for the correct material is essential for the damage-mitigating control synthesis. The remaining part of this section presents the results of γ-parameter fitting based on the experimental data (Swain et al., 1990) for the material AISI 4340 steel.

Table 1 Effective stress intensity factor range versus crack growth rate relationship

ΔK_{eff} Mpa $\sqrt{m}$	da/dN m/cycle
3.75	3.0E-10
5.30	2.0E-09
7.30	7.0E-09
15.00	4.5E-08
50.00	5.5E-07
120.00	3.0E-05

In the model of Newman et al. (1981), the stress intensity factor range ΔK used in the Paris equation is replaced by effective stress intensity factor range ΔK_{eff}. The crack opening stress is determined by a crack closure model which is similar to the Dugdale model (Dugdale, 1960) but it is modified to leave plastically deformed material in the wake of the advancing crack tip. In the present paper, however, we have computed the crack opening stress by simplified equations (Newman, 1984) which are obtained through curve fitting based on the original model. The experiments show that a unified approach (Newman et al., 1992) based on the crack closure concept can be used for damage prediction starting from the initial defect (microcrack) to the failure of materials without significant errors. A relationship between the effective stress intensity factor range and crack growth rate obtained from the experimental data of AISI 4340 Steel is given in Table 1 (Swain et al., 1990).

In Table 1, the values of ΔK_{eff} and da/dN are linearly interpolated between two consecutive data points using the logarith-

Table 2 Material properties of AISI 4340 steel

Young's modulus (E)	193500 N/mm^2
Yield strength, monotonic (σ_y)	1374 N/mm^2
Yield strength, cyclic (σ_y')	905 N/mm^2
Cyclic-strength coefficient (K')	1890 N/mm^2
Cyclic-strength hardening exponent (n')	0.118
Fatigue-strength coefficient (σ_f')	1880 N/mm^2
Fatigue-strength exponent (b)	−0.086
Fatigue-ductility coefficient (ϵ_f')	0.706
Fatigue-ductility exponent (c)	−0.662

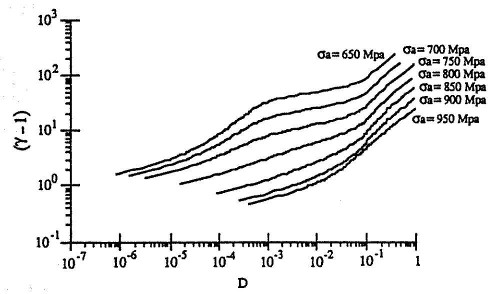

Fig. 8 γ **versus** D **at different stress amplitudes**

mic scale while those beyond the maximum and minimum are extrapolated. The initial crack size is identified based on the assumption that the fatigue life predicted by the strain life approach is equal to that obtained via the crack closure model. The damage, in this case, is defined as the normalized crack length with respect to its critical length to failure, i.e., $D = a/a^*$ where the critical crack length a^* is obtained from fracture toughness of the material. The material and fatigue properties of AISI 4340 steel are given in Table 2 (Boller and Seeger, 1987).

The results of the nonlinear damage D versus the linear damage δ which is essentially the cycle ratio are used to compute γ from Eq. (21). Figure 8 shows the relationship between γ and D for different values of the (constant) stress amplitude σ_a as a series of curves in the logarithmic scale. If these curves are generated to be closely spaced, the values between two curves can be obtained via linear interpolation without an appreciable error. Once the γ-parameters are computed as a function of two independent variables $\Delta\sigma$ and D, the nonlinear damage model described above can be readily used to predict the nonlinear damage behavior at different stress amplitudes.

4 Summary and Conclusions

Although a significant amount of research has been conducted in the individual areas of *control and diagnostics* and *analysis and prediction of materials damage*, integration of these two disciplines has not received much attention. We have proposed, in this paper, fatigue damage representation of the critical components as an augmentation to control and diagnostics of complex dynamic processes such as advanced aircraft, spacecraft, and power plants. Since the model parameters strongly depend on the type of the material, availability of pertinent experimental data for the correct material is essential for fatigue damage prediction and control synthesis. The key idea is to achieve high performance without overstraining the mechanical structures such that the functional life of critical components is increased resulting in enhanced safety, operational reliability, and availability. Efficacy of the proposed damage-mitigating control has been tested in the second part (Ray et al., 1994) via simulation of transient operations of a reusable rocket engine.

The proposed damage-mitigating control of mechanical systems has a wide spectrum of potential engineering applications. Examples are reusable rocket engines for space propulsion, rotating and fixed wing aircraft, fossil and nuclear plants for electric power generation, automotive and truck engine/transmission systems, and large rolling mills. In each of these systems, damage-mitigating control can enhance service life, safety and productivity. Extended life coupled with enhanced safety and high performance is expected to have a significant economic impact in diverse industrial applications.

Acknowledgments

The authors acknowledge benefits of discussion with Professor D. A. Koss regarding the metallurgical aspects of this research work, and technical contributions of Dr. L-W. Liou during the initial phase of this project.

APPENDIX A

Modeling of Integrated Fatigue-Creep-Corrosion Damage

The contributions of creep and corrosion on structural damage become significant at elevated temperatures (as low as about 30 percent of the melting point of the material in some cases) due to the effects on micromechanisms of fatigue fracture. For example, the fatigue failure at a low temperature usually results from transgranular fracture but it may occur due to intergranular fracture at an elevated temperature.

Although the time-dependent part of the fatigue-creep damage is thermally activated and results from both creep and corrosion in gaseous and aqueous environments, linear elastic fracture mechanics can frequently be used for damage prediction provided that the stress intensity factor range remains the controlling parameter for crack propagation. This is valid if the zone of inelastic deformation at the crack tip is small in size compared to the uncracked length. However, at very high temperatures and low cycles (for example, cooling tubes of the main combustion chamber in rocket engines, or overheated tubes of steam generators), the elastic failure mechanism may not be prevalent as the inelastic zone becomes appreciably large. Furthermore, the material properties such as the tensile strength and fracture toughness change significantly at elevated temperatures relative to their nominal values. The dynamics of creep damage may be modeled from these perspectives. The total strain rate $\dot{\epsilon}$ consisting of elastic strain rate $\dot{\epsilon}_e$ and plastic strain rate $\dot{\epsilon}_p$ is modeled for a viscoplastic material under uniaxial tension in terms of the instantaneous stress σ and the stress rate $\dot{\sigma}$ as (Lemaitre, 1992):

$$\dot{\epsilon} = \dot{\epsilon}_e + \dot{\epsilon}_p \text{ where } \dot{\epsilon}_e = \frac{\dot{\sigma}}{\mathrm{E}} \text{ and } \dot{\epsilon}_p = \left(\frac{\sigma}{\sigma_y}\right)^{n_c} \quad \text{(A.1)}$$

The material parameters are: Young's modulus E; yield strength σ_y; and power law creep exponent n_c. Equation

(A.1) may have to be modified for multi-axial stress conditions in the critical components. In that case, the effective stress needs to be defined as a function of the stress tensor.

Some investigators, for example (Saxena, 1988), have computed the total damage as the sum of corrosion-fatigue and creep damages that are obtained independently. That is, the cumulative damage D_{cf} in creep-fatigue cycling has been defined upon completion of n cycles as:

$$D_{cf} = D_f + D_c \tag{A.2}$$

where D_f is the fatigue damage part; D_c is the creep damage part; and D_{cf} is normalized to unity at the onset of failure. Similar to the linear damage rule for cumulative fatigue damage, the creep damage is often based on time summation as:

$$D_c = \sum_{i=1}^{n} \left\{ N_{fh} \int_0^{t_h} \frac{dt}{t_r} \right\}_i \tag{A.3}$$

where N_{fh} is the number of cycles to failure in creep-fatigue; t_r is the time to creep-rupture, and t_h is the hold time. Based on the observed failure models for the creep-fatigue interaction, ductility is considered to have a major influence on failure of engineering materials. Zamrik and Davis (1990) have proposed a model of the creep damage part D_c based on the ductility exhaustion concept as follows:

$$D_c = \sum_{i=1}^{n} \left\{ N_{th} \int_0^{t_h} \left[\frac{\Delta \dot{\epsilon}_{cp}}{\vartheta(\Delta \dot{\epsilon}_{cp})} \right] dt \right\}_i \tag{A.4}$$

where $\Delta\dot{\epsilon}_{cp}$ is the rate of creep strain range during the hold-time period, and $\vartheta(\Delta\dot{\epsilon}_{cp})$ is the material creep ductility as a function of $\Delta\dot{\epsilon}_{cp}$. If the creep strain accumulation during the hold-time period is assumed to obey the power law, then

$$\Delta \dot{\epsilon}_{cp} = A(\Delta\sigma)^q t^{r-1} \tag{A.5}$$

where A, r and q are constants, and $\Delta\sigma$ is the stress range at time t during hold period. Pineau (1989) also proposed a ductility exhaustion model where the creep damage D_c is expressed in terms of the instantaneous values of plastic strain rate $\dot{\epsilon}_p$, stress σ, and temperature T as:

$$D_c(t) = \int_0^t \left(\frac{\dot{\epsilon}_p(\sigma(\tau),T(\tau))}{\dot{\epsilon}_s(\sigma(\tau),T(\tau))} \right) \times \frac{d\tau}{t_r(\sigma(\tau),T(\tau))} \tag{A.6}$$

where t is the current time, and $\dot{\epsilon}_s$ is the stationary creep rate (Coutsouradis et al., 1978). The two models in Eqs. (A.5) and (A.6) need to be solved in view of the fact that ductility is the primary parameter for creep damage at elevated temperatures.

Modeling of corrosion-fatigue crack growth in gaseous environments has been reported by several investigators including Wei (1989). The governing equations for damage dynamics are formulated on the basis of mass balance and reaction kinetics where the state variables are gas pressure at the crack tip and percent of surface reactions. In general, the corrosion-fatigue crack growth rate $(da/dN)_{cf}$ can be obtained as a modification of the pure fatigue rate $(da/dN)_f$ by including the states of gas pressure and surface reactions. The dynamics of corrosion are likely to be slow relative to fatigue dynamics except for operations at elevated temperatures. Depending on the operating conditions, it might be possible to eliminate the above state variables by varying the parameters of the fatigue crack growth equation slowly with time. Therefore, the constraint parameters β and Γ in Eqs. (4) and (5) may also be chosen as slowly varying functions of time to incorporate the effects of corrosion.

Following the procedures described in Sections 3.1 and 3.2, the cycle-dependent corrosion-fatigue crack growth rate $(da/dN)_{cf}$ can be converted to the time-dependent crack growth rate $(da/dt)_{cf}$. The corrosion-fatigue damage is defined, similar to Eq. (B.1) in Appendix B, as $D_{cf} = a/a^*$ where a^* is the critical crack length. Then, following the structure of Eq. (2), a dynamic model of the combined effects of creep and fatigue damage at a single critical point is proposed as follows:

$$\frac{dD_{cf}}{dt} = h_{cf}(D_{cf}(t), D_{cr}(t), q(x,t),,t);$$
$$D_{cf}(t_0) = D_{cf0};\ h_{cf} \geq 0\ \forall t \tag{A.7}$$

$$\frac{dD_c}{dt} = h_{cr}(D_{cf}(t), D_{cr}(t), q(x,t),t);$$
$$D_{cr}(t_0) = D_{cr0};\ h_{cr} \geq 0\ \forall t \tag{A.8}$$

In the above equation set, the damage vector is expressed as $v(t) = [D_{cf}\, D_c]^T$. For multiple critical points, the damage vector includes the damage components at all points. Finally, a scalar measure D of total damage is expressed as a function of the corrosion-fatigue damage and creep damage, and the end of service life occurs at $D = 1$.

APPENDIX B

Modeling of Fatigue Damage Via Linear Elastic Fracture Mechanics Approach

The concept of a continuous-time damage model, developed in Section 3 using the strain-life approach, can be extended to formulate a continuous-time damage model for crack propagation as explained below.

In the most commonly used fatigue crack models (e.g., Paris model and Forman model (Bannantine et al., 1990)), the growth rate of the crack length, a, relative to the number of cycles, N, is directly dependent on the stress intensity factor range ΔK. We propose to follow the concept of the crack closure model (Newman, 1981) and therefore ΔK is replaced by the effective stress intensity range ΔK_{eff}. To be consistent with the strain-life approach, damage is assumed to be identically equal to 1 at the onset of component failure, i.e., when the crack length, a, reaches the critical value, a^*, which can be estimated from the fracture toughness of the material. The damage is assumed to occur only if the instantaneous stress is increasing and the crack opening stress σ_0 is exceeded. This implies that the damage rate is equal to zero during unloading. The damage increment, denoted as ΔD_f, during the rising reversal can be expressed as a function of σ, σ_0, and D_f.

$$\Delta D_f = \frac{dD_f}{dN} = \frac{1}{a^*} \times \frac{da}{dN} = \frac{1}{a^*} F(\sigma,\sigma_0,a^* D_f) \tag{B.1}$$

where the fatigue damage is defined as $D_f = a/a^*$ in the absence of a more precise definition of damage. Since the damage increment ΔD_f is relatively small, the total damage D_f is assumed to remain constant during a reversal. The damage rate can be obtained by differentiating Eq. (B.1) with respect to time.

$$\frac{dD_f}{dt} = \left(\frac{1}{a^* - \dfrac{\partial F}{\partial D_f}} \right) \frac{\partial F}{\partial \sigma} \frac{d\sigma}{dt} \tag{B.2}$$

References

Bannantine, J. A., Comer, J. J., and Handrock, J. L., 1990, *Fundamentals of Metal Fatigue Analysis,* Prentice Hall.

Boller, C., and Seeger, T., 1987, *Materials Data for Cyclic Loading,* Elsevier.

Bolotin, V. V., 1989, *Prediction of Service Life for Machines and Structures,* ASME.

Courtney, T. H., 1990, *Mechanical Behavior of Materials,* McGraw-Hill, New York, NY.

Coutsouradis, D. et al., eds., 1978, *High Temperature Alloys for Gas Turbines,* Applied Science, London, p. 513.

Dowling, N. E., 1983, "Fatigue Life Prediction for Complex Load Versus Time Histories," ASME *Journal of Engineering Materials and Technology,* Vol. 105, pp. 206–214.

Dugdale, D. S., 1960, "Yielding of Steel Sheets Containing Slits," *Journal of Mechanics, Physics, and Solids,* Vol. 8, pp. 100–104.

Hertzberg, R. W., 1989, *Deformation and Fracture Mechanics of Engineering Materials,* John Wiley, New York, NY.

Kwakernaak, H., and Sivian, R., 1972, *Linear Optimal Control Systems,* Willey-Interscience, New York, NY.

Lemaitre, J., 1992, *A Course on Damage Mechanics,* Springer-Verlag, Berlin.

Lorenzo, C. F., and Merrill, W. C., 1991a, "An Intelligent Control System for Rocket Engines: Need, Vision and Issues," *IEEE Control Systems Magazine,* Vol. 11, No. 1, June, pp. 42–46.

Lorenzo, C. F., and Merrill, W. C., 1991b, "Life Extending Control: A Concept Paper," American Control Conference, Boston, MA, June, pp. 1080–1095.

Manson, S. S., and Halford, G. R., 1981, "Practical Implementation of the Double Linear Damage Rule and Damage Curve Approach for Treating Cumulative Fatigue Damage," *Int. Journal of Fracture,* Vol. 17, No. 2, pp. 169–192.

Marco, S. M., and Starkey, W. L., 1954, "A Concept of Fatigue Damage," *Trans. ASME,* Vol. 76, No. 4, pp. 627–632.

Newman, J. C., Jr., 1981, "A Crack Closure Model for Predicting Fatigue Crack Growth under Aircraft Spectrum Loading," *Methods and Models for Predicting Fatigue Crack Growth under Random Loading,* ASTM STP 748, pp. 53–84.

Newman, J. C., Jr., 1984, "A Crack Opening Stress Equation for Fatigue Crack Growth," *Int. Journal of Fracture,* Vol. 24, pp. R131–R135.

Newman, J. C., Jr., Phillips, E. P., Swain, M. H., and Everett, Jr., R. A., 1992, "Fatigue Mechanics: An Assessment of A Unified Approach to Life Prediction," *ASTM Symposium On Advances in Fatigue Lifetime Predictive Techniques,* ASTM STP 1122, M. R. Mitchell and R. W. Landgraf, eds., American Society for Testing Materials, Philadelphia, pp. 5–27.

Noll, T., Austin, E., Donley, S., Graham, G., Harris, T., Kaynes, I., Lee, B., and Sparrow, J., 1991, "Impact of Active Controls Technology on Structural Integrity," *32nd AIAA/ASME/ASCE/AHS/ASC Structures, Structural Dynamics, and Materials Conference,* Baltimore, MD, Apr., pp. 1869–1878.

Paris, P. C., and Erdogan, F., 1963, "A Critical Analysis of Crack Propagation Laws," ASME *Journal of Basic Engineering,* Vol. 85, pp. 528–534.

Pineau, A., 1989, "Elevated Temperature Life Prediction Methods," *Advances in Fatigue in Science and Technolgoy,* C. M. Branco and L. G. Rosa, eds., Proceedings of NATO ASI Series, Kluwer Academic, Dordrecht, pp. 313–338.

Ray, A., Wu, M-K., Carpino, M., and Lorenzo, C. F., 1993, "Damage-Mitigating Control of Mechanical Systems: Part II—Formulation of an Optimal Policy and Simulation," published in this issue, pp. 448–455.

Royden, H. L., 1988, *Real Analysis,* 3rd edition, Macmillan Publishing Company, New York, NY.

Saxena, A., 1988, "A Model for Predicting the Effect of Frequency on Fatigue Crack Growth at Elevated Temperature," *Fatigue of Engineering Materials and Structures,* Vol. 3, pp. 247–255.

Sobczyk, K., and Spencer, B. F., Jr., 1992, *Random Fatigue: Data to Theory*, Academic Press, Boston, MA.

Suresh, S., 1991, *Fatigue of Materials*, Cambridge University Press, Cambridge, U.K.

Swain, M. H., Everett, R. A., Newman, J. C., Jr., and Phillips, E. P., 1990, "The Growth of Short Cracks in 4340 Steel and Aluminum-Lithium 2090," *AGARD Report,* No. 767, pp. 7.1–7.30.

Tucker, L., and Bussa, S., 1977, "The SAE Cumulative Fatigue Damage Test Program," *Fatigue Under Complex Loading: Analyses and Experiments,* Vol. AE-6, pp. 1–54.

Vidyasagar, M., 1992, *Nonlinear Systems Analysis*, 2nd ed., Prentice Hall, Englewood Cliffs, NJ.

Wei, R. P., 1989, "Environmentally Assisted Fatigue Crack Growth," *Advances in Fatigue in Science and Technology,* C. M. Branco and L. G. Rosa, eds., Proceedings of NATO ASI Series, Kluwer Academic, Dordrecht., Germany.

Wheeler, O. E., 1972, "Spectrum Loading and Crack Growth," ASME *Journal of Basic Engineering,* Vol. 94, pp. 181–186.

Willenborg, J., Engle, R. M., and Wood, H. A., 1971, "A Crack Growth Retardation Model Using an Effective Stress Concept," AFFDL TM-71-1-FBR, Air Force Flight Dynamics Lab. Jan.

Wu, M-K., 1993, "Damage-Mitigating Control of Mechanical Systems," Ph.D. dissertation in Mechanical Engineering, The Pennsylvania State University, University Park, PA.

Zamrik, S. Y., and Davis, D. C., 1990, "Creep-Fatigue Damage Mechanisms and Life Assessment of Two Materials: Type 316 Stainless Steel and Waspalloy," ASM International Conference on Life Assessment and Repair Technology for Combustion Turbine Hot Section Components, April 17–19, Phoenix, AZ.